Silicoflagellates and *Actiniscus*:
Vertical Fluxes at Pacific and Atlantic Sediment Trap Stations

Kozo Takahashi

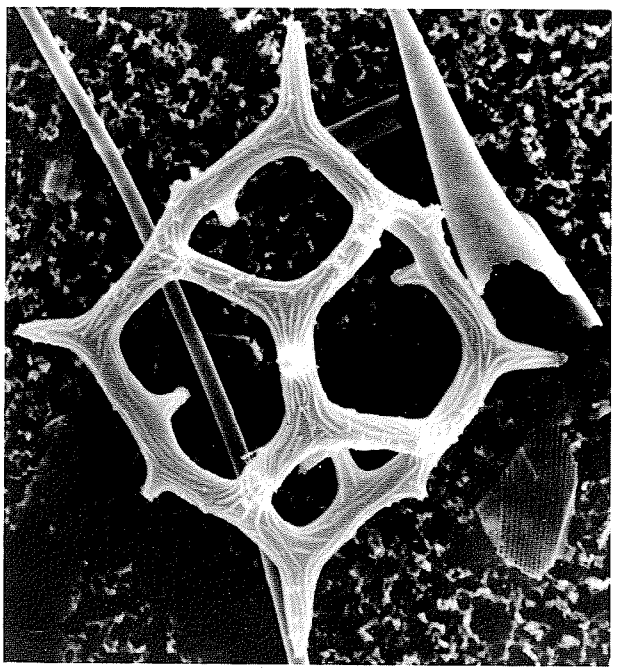

Edited by

Susumu Honjo

Woods Hole Oceanographic Institution
Woods Hole Massachusetts 02543
U.S.A

Ocean Biocoenosis Series No. 2

Silicoflagellates and *Actiniscus*: Vertical Fluxes at Pacific and Atlantic Sediment Trap Stations

Kozo Takahashi
Department of Geology and Geophysics
Woods Hole Oceanographic Institution
Woods Hole, MA 02543

Edited by

Susumu Honjo

Woods Hole Oceanographic Institution
Woods Hole Massachusetts 02543
U.S.A

Ocean Biocoenosis Series No. 2

Ocean Biocoenosis Series No. 2
Woods Hole Oceanographic Institution, Woods Hole, MA 02543

Published 1991
Printed in the United States of America

Availability: Office of the Research Librarian
Woods Hole Oceanographic Institution
Woods Hole, Massachusetts 02543
U.S.A.

$10.00 U.S.

ISBN 1-880224-01-1

Explanation of Cover Photo: A scanning electron photomicrograph of *Dictyocha mandrai* Ling collected by one (7–22 November, 1982) of the time-series PARFLUX sediment traps placed at 3,800 m depth at Station PAPA (50°N, 145°W) in the Gulf of Alaska. *D. mandrai* is commonly found in many parts of the world oceans. The basal ring diameter (major axis) of this specimen is 45 μm.

Contents

List of Tables

List of Figures

Silicoflagellates and *Actiniscus*: Vertical Fluxes at Pacific and Atlantic Sediment Trap Stations

Kozo Takahashi

Abstract

Vertical fluxes of silicoflagellate skeletons were measured in meso- and bathypelagic zones at four PARFLUX sediment trap stations located in the Pacific and Atlantic oceans. The average flux measured at several depths ranged from 35 × 10^3 skeletons/m^2/day at the Pacific gyre (P_1) station to 424 × 10^3 skeletons/m^2/day at the Panama Basin (PB_1) station. The skeletal fluxes at these stations constituted a few weight percent or less of the total biogenic opal flux.

The fluxes measured at Station P_1, as well as the relative abundance of different assemblages, were fairly constant with depth. At Station PB_1, while relative abundance of assemblages was constant with depth, the flux measured at mesopelagic depths was threefold greater than that in the bathypelagic zone. At equatorial Atlantic Station E a slight increase toward the bathypelagic zone is correlated with gradual change in the relative abundance of two predominant taxa, suggesting seasonality in the production of each taxa. Aggregate forms of vertical settling were observed at Station E; the number of skeletons in the aggregates was more than one-half of the total number in the mesopelagic zone and it decreased with increasing depth.

The percent abundances of Dictyocha messanensis messanensis *and* Distephanus pulchra *are correlated with organic carbon flux at four stations. Preservation of the skeletons in Holocene sediment at Station P_1 is less than one percent of the silicoflagellate flux.*

Introduction

Silicoflagellates, chrysophyton phytoplankton, are ubiquitous in most parts of the world's oceans, including neritic to pelagic environments, and are known to occur most abundantly in eutrophic waters (e.g., Kozlova and Mukhina, 1967). Their cell size commonly ranges from 20 to 80 μm in diameter and therefore they are classified as microplankton. Their skeletons are made of hollow siliceous tubes. The biology of living silicoflagellates is summarized in Lipps (1970). Although silicoflagellate skeletons generally constitute a relatively minor component in marine sediments, scientists have successfully utilized silicoflagellate skeletons for biostratigraphy in many parts of the oceans, especially where calcareous fossils are absent. The fossil record of the silicoflagellate skeletons is known since the Late Cretaceous; silicoflagellate stratigraphy for the Maestrichtian to Quaternary period has been summarized in Bukry (1981).

A number of authors have used fossil silicoflagellate assemblages to make paleotemperature estimates (e.g., Mandra, 1969; Shitanaka et al., 1970; Poelchau, 1974; Ciesielski, 1975; Ling, 1975; Bukry, 1977). The application of skeletal abundance to paleoproductivity requires a better understanding of spatial and temporal variability of living silicoflagellate species.

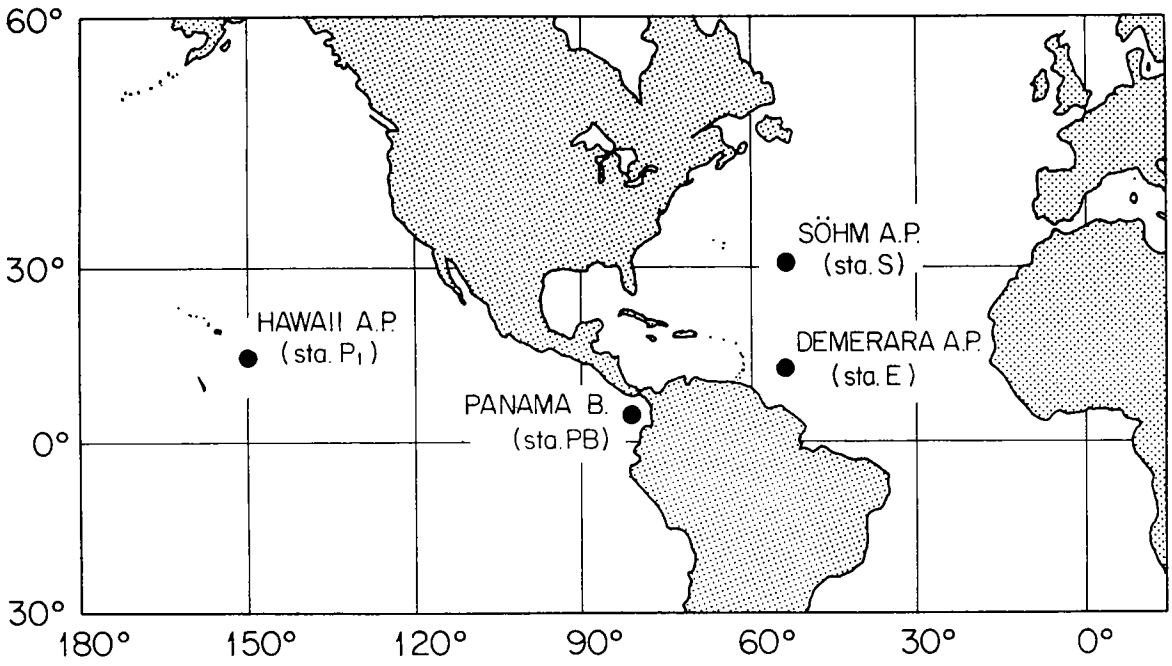

Figure 1: Location of the PARFLUX sediment trap stations.

While studies on silicoflagellates from the upper water column have contributed to an understanding of distribution (Nival, 1965; Kozlova and Mukhina, 1967; O'Kane, 1970; Murray and Schrader, 1983), detailed information on silicoflagellate sedimentation processes is meager. Sediment trapping is an efficient method for collecting sinking particles in the water column (e.g., Honjo, 1978, 1980; Brewer et al., 1980; Bruland et al., 1981) and thus one should be able to measure modern sedimentation rates which can be directly compared with underlying sediments. In this paper a study of silicoflagellate fluxes is reported, based on examination of sediment trap material collected over two- to four-month periods and recovered from the Atlantic and Pacific PARFLUX stations (Figure 1).

Actiniscus pentasterias (Ehrenberg) (1841) is a species of dinoflagellate that is known to produce siliceous endoskeletons in the present-day oceans (Orr and Conley, 1976: Plate 2, figures 12 to 15 of this paper). Because it is siliceous and similar in size range to silicoflagellate skeletons, it is included in this paper. No ebridians were encountered in the set of samples studied here.

Source of Samples, Methods of Analysis

All of the 14 samples used in this study were recovered from PARFLUX sediment traps deployed in the Atlantic and Pacific (Figure 1). Details of the recovery of the trap samples are discussed by Honjo (1980). Briefly, the sediment trap array consisted of four or five traps, model PARFLUX Mark II with 1.5 m^2 opening (Honjo et al., 1980), which were moored at several depths for 2 to 4 months (Table 1). The receiving cups were sealed by a time-controlled spring shutter prior to recovery.

Table 1: Summary of the sample sources from the PARFLUX sediment traps deployed in the Atlantic and Pacific.

	PARFLUX S_2	PARFLUX E	PARFLUX P_1	PARFLUX PB_1
Location	31°32.5′N 55°55.4′W	13°30.2′N 54°00.1′W	15°21.1′N 151°28.5′W	05°21′N 81°53′W
Ocean/Basin	Central Sargasso Sea/ Söhm Abyssal Plain	Tropical Atlantic/ Demerara Abyssal Plain	N. Central Pacific/ E. Hawaii Abyssal Plain	Tropical Pacific/ hemipelagic Panama Basin
Term	7/77–10/77	11/77–2/78	9/78–11/78	8/79–12/79
Duration	110 days	98 days	61 days	112 days
Trap Depth (m)	976	389 988 — 3,775 5,068	378 978 2,778 4,280 5,582	667 1,268 2,869 3,769 3,791
Anchor Depth (m)	5,581	5,288	5,792	3,856

Since the same sample slides were used for both silicoflagellate and radiolarian studies, the sample preparation technique for preparing silicoflagellate slides was the same as described in the radiolarian paper of the Ocean Biocoenosis Series (Takahashi, in press). The wet samples, after passing through a 1 mm screen, were split into four aliquots using an Honjo/Erez precision rotary liquid splitter (Honjo, 1978, 1980). Further splitting was repeated until an appropriate sample size was obtained; an aliquot that has been diluted enough so that specimens can be well observed under the transmission light microscope and yet dense enough to maintain counting efficiency within a slide. Typically, an original sample was split six times to obtain 1/4096 aliquot. The resulting aliquot was wet sieved through 250, 125, and 63 μm screens. When necessary, the samples were split further to smaller aliquots prior to filtration. Samples from Station E of less than 63 μm fraction were independently prepared using a dilution method (Takahashi and Honjo, 1981); a 1/64 aliquot was diluted to 250 ml in a measuring flask and then a 2-ml aliquot was taken by use of a pipet.

The above aliquots were filtered through a 47 mm (diameter) HA Millipore© filter (grid printed) with a nominal 0.45 μm pore size using a rectangular filtration funnel with a 19 × 42 mm opening. The residue was rinsed with distilled water, dried at 50°C in an oven and mounted on a standard glass slide with Cargile© type B compound (refractive index = 1.5150) in order to clear the sample filter. A few days later when bubbles have escaped from the sample, a cover glass was set in place with a 5-minute epoxy glue on two corners. The aliquot size used and number of slides counted for each sample is listed in Table 2. Counts of four size fractions (1.000–250, 250–125, 125–63, and <63 μm) were combined to give a flux value for a sample. In the case of station P_1 three size fractions (1,000–250, 250-63 and <63 μm) were counted (Table 2).

Table 2: Size of aliquot in each microslide relative to total sediment trap sample. Number of slides used for counts is one, otherwise presented in footnotes.

Station:	Depth (m)	Size Fraction 1000–250 (μm)	250–125 (μm)	125–63 (μm)	< 63 (μm)
E:	389	1/256	1/1024	1/1024	1/8000
	988	1/256	1/1024	1/1024	1/8000
	3755	1/256	1/1024	1/1024	1/8000
	5068	1/256	1/1024	1/1024	1/8000
PB_1:	667	1/4096	1/1024	1/1024	1/16384[a]
	1268	1/1024	1/1024	1/1024	1/4096
	2869	1/4096	1/1024	1/1024	1/16384
	3769[b]	1/4096	1/4096	1/4096	1/16384
	3791	1/1024	1/1024	1/1024	1/16384

[a]Two slides were used for count.
[b]Additional counts were made on slides of 250–125 μm and 125–63 μm.

Station:	Depth (m)	Size Fraction 1000–250 (μm)	250–63 (μm)	< 63 (μm)
P_1:	378	1/256	1/256	1/256
	978	1/256	1/256	1/256
	2778	1/256	1/256[a]	1/1024
	4280	1/256	1/256[a]	1/1024
	5582	1/256	1/256	1/1024

[a]Additional counts were made on slides of 250–125 μm and 125–63 μm.

The slides were studied to identify and count silicoflagellate species under a transmission compound light microscope at magnifications of 100 and/or 400 times. Double skeletons, that occur during vegetative reproduction, were rarely encountered and were counted as two skeletons. With the exception of a few cases, all skeletons were intact. The whole area of each slide taken from stations E and S_2 samples was examined during census taking. However, for samples from other stations only five vertical transverses were examined for census purposes and an extrapolation was made in order to estimate the number of silicoflagellates in each sample. The five transverses correspond to 5 and 28 percent of the entire area of a slide at 400× and 100× magnification, respectively. The justification for assuming that the counts found in five transverses are adequate is as follows. Counts of ten distantly separated transverses from one end to the other were made using a dozen separate slides from Station PB_1. There was a tendency toward finding slightly higher values in the transverses of the central area than those found in the marginal areas of the slides. A similar tendency was also reported in diatom counts in an independent study (Schrader and Gersonde, 1978). F tests indicated that there was no significant difference in standard deviations between random 5 and 10 transverse groups. Thus, it was concluded that 5 transverses were adequate for silicoflagellate counts for the slides prepared in this study. The standard deviations were commonly about 13% with the maximum being 17%. The maximum value is about equal to or less than standard deviations of silicoflagellate counts using several slides from the same sample; commonly 15% to 20% and a maximum of 25%. Therefore, experimental errors encountered in this study including splitting and counting, but excluding sediment trapping efficiency which has been discussed elsewhere (Brewer et al., 1980), were less than about 25%. Actual counts of each size fraction are listed in Table 3.

Scanning electron microscopy (SEM) preparation was similar to that used for the Radiolarian paper in the Ocean Biocoenosis Series (Takahashi, in press). A small portion of the sample dry filter was cut and mounted with a drop of conductive paint on an aluminum stub, then coated with carbon, then with Pd-Au film.

Dimensions of the major basal ring was measured in a transmission microscope-based video system at a magnification of 400 times with systematic errors of 1.5 μm or less. The major basal ring is defined as the distance between the central points of junctions of the basal ring and the polar radial spines. The number of specimens (n) used for size measurements ranged from 22 to 120 skeletons.

Systematics

Most taxonomic nomenclature of silicoflagellates is based on the skeletal material collected from the sea-floor and which is already subjected to selective dissolution and diagenesis. Little taxonomic work has been done on silicoflagellates collected from the water column (Poelchau, 1974). In this chapter, all species recovered from sediment traps deployed at four tropical and temperate stations during different seasons are examined with the hope that the results will contribute to improving the classifications. Morphological terminology used in this report is that of Poelchau (1976).

Table 3: Size fractioned fluxes (skeletons/m^2/day) of silicoflagellates from PARFLUX sediment trap stations. Note that at Station P_1 a different size fraction (250–63 μm) was used. Data for total and three major species are presented. Actual counts of silicoflagellates (Number Skeletons/Slide) are given in the far right column.

Station: and Depth (m)	Size Fraction (μm)	Total Silicoflagellates	*Dictyocha messanensis spinosa*	*Dictyocha messanensis messanensis*	*Distephanus pulchra*	Number Skeletons/Slide
E: 389	1,000–250	8,896	6,141	2,720	0	7,558
	250–125	11,605	7,746	3,817	14	2,821
	125–63	9,487	6,060	3,274	21	1,906
	< 63	62,313	41,469	20,245	0	1,228
988	1,000–250	3,800	2,368	1,397	0	3,360
	250–125	2,173	1,379	787	0	510
	125–63	2,982	1,672	1,226	0	649
	< 63	94,639	43,755	49,415	163	1,768
3,755	1,000–250	3,885	2,107	1,724	0	2,984
	250–125	738	320	390	7	138
	125–63	5,824	3,218	2,327	21	950
	< 63	201,035	94,803	104,381	218	3,724
5,068	1,000–250	5,339	2,515	2,713	7	3,700
	250–125	2,285	1,038	1,191	7	410
	125–63	1,707	1,303	334	14	367
	< 63	140,734	51,537	87,401	109	2,607
P_1: 378	1,000–250	123	0	92	31	13
	250–63	135	0	115	20	13
	< 63	873	0	596	277	23
978	1,000–250	268	0	176	92	27
	250–63	593	11	425	157	57
	< 63	9,851	78	7,230	2,543	250
2,778	1,000–250	447	53	383	11	45
	250–63	943	53	663	227	93
	< 63	30,182	313	28,918	951	194
4280	1,000–250	156	11	145	20	15
	250–63	993	42	744	53	97
	< 63	48,782	1,432	41,475	1,108	318
5,582	1,000–250	320	21	268	31	31
	250–63	644	52	478	114	62
	< 63	29,075	1,088	23,478	3,887	187
PB_1: 667	1,000–250	61,853	5,266	10,703	39,253	2,536
	250–125	38,350	4,547	7,875	21,077	886
	125–63	55,971	7,387	14,037	26,685	1,288
	< 63	718,313	75,484	173,446	389,364	1,567
1,268	1,000–250	18,481	1,658	3,182	12,069	1,516
	250–125	35,657	5,108	8,917	16,616	412
	125–63	38,338	5,455	6,662	21,723	443
	< 63	190,051	21,821	37,035	104,546	549
2,869	1,000–250	32,451	3,340	5,291	20,114	350
	250–125	24,326	3,724	4,157	12,983	281
	125–63	25,362	4,590	3,633	12,202	293
	< 63	258,926	16,579	52,663	160,622	187
3,769	1,000–250	5,583	536	805	3,974	62
	250–125	8,948	1,438	2,170	4,340	99
	125–63	7,753	1,365	1,707	4,145	86
	< 63	274,238	33,256	33,256	153,698	208
3,791	1,000–250	6,070	610	1,286	3,358	269
	250–125	6,862	926	1,694	3,407	304
	125–63	22,241	4,846	4,760	8,485	257
	< 63	290,816	24,966	78,897	145,408	210
S_2: 976	250–125	17,576	1,043	16,136	0	2,832

Division CHRYSOPHYCOPHYTA
Class CHRYSOPHYCEAE
Subclass SILICOFLAGELLATOPHYCIDAE BORGERT
Order SIPHONOTESTALES LEMMERMANN
Family DICTYOCHIDAE LEMMERMANN
Genus *Dictyocha* EHRENBERG, 1837

Dictyocha messanensis Haeckel *spinosa* LEMMERMANN
Plate 1, figures 2–4, 15

Dictyocha messanensis HAECKEL, 1861, pp. 799–800; 1862, p. 272, pl. 12, figs. 3–6. DUMITRICA, 1972, p. 907, pl. 8, figs. 8–13, pl. 9, figs. 2–4. LING, 1977, p. 207. MURRAY AND SCHRADER, 1983, pl. I, fig. 19 (partim.).

Dictyocha fibula var. *messanensis* (Haeckel). LING, 1970, p. 92, pl. 18, fig. 14.

Dictyocha fibula var. *messanensis* forma *spinosa* LEMMERMANN, 1908, p. 28, fig. 95.

Dictyocha messanensis forma *spinosa* Lemmermann. POELCHAU, 1976, p. 174, p. 5, figs. b, e, f.

See Ling (1970), Dumitrica (1972) and Poelchau (1976) for a more complete list of synonymies.

DESCRIPTION: Basal ring is usually rhombic and occasionally square. Basal bars straight or slightly convex. Radial spines are about one half of basal ring diameter; two polar radial spines longer than equatorial ones. Apical bar is usually 1/2 to 3/4 length of major basal ring diameter and convex, with a conical apical spine straight upward. An axis of the apical bar is offset from that of radial spines at two poles by about 10° (8–13°). Lateral rods are convex, with or without lateral spines, and with accessory micro-spines.

DIMENSIONS: Major basal ring diameter 24–39 μm (Figure 2).

REMARKS: Apparently the present taxon is identical with *D. messanensis* forma *spinosa* Lemmermann illustrated by Poelchau (1976). Also, a specimen illustrated as *D. messanensis* by Murray and Schrader (1983, pl. I, fig. 19) is the same as the present taxon. Specimens of *D. messanensis* illustrated by Dumitrica (1972) are much smaller in size than those illustrated by Ling (1970). The specimens studied here correspond to a size intermediate between those cited by the above two authors. It is possible that the size of *D. messanensis spinosa* varies widely depending on environmental factors as well as taxonomic criteria. Although a distinction between quadrate and pentagonal forms was made during the census (Table 4), these two forms are tentatively considered as a single species. A t test suggests that major basal ring diameters of different populations of this species are similar to one another in samples from stations S_2, E, and PB_1, but those from Station P_1 are significantly different from the rest (Figure 2, Table 4).

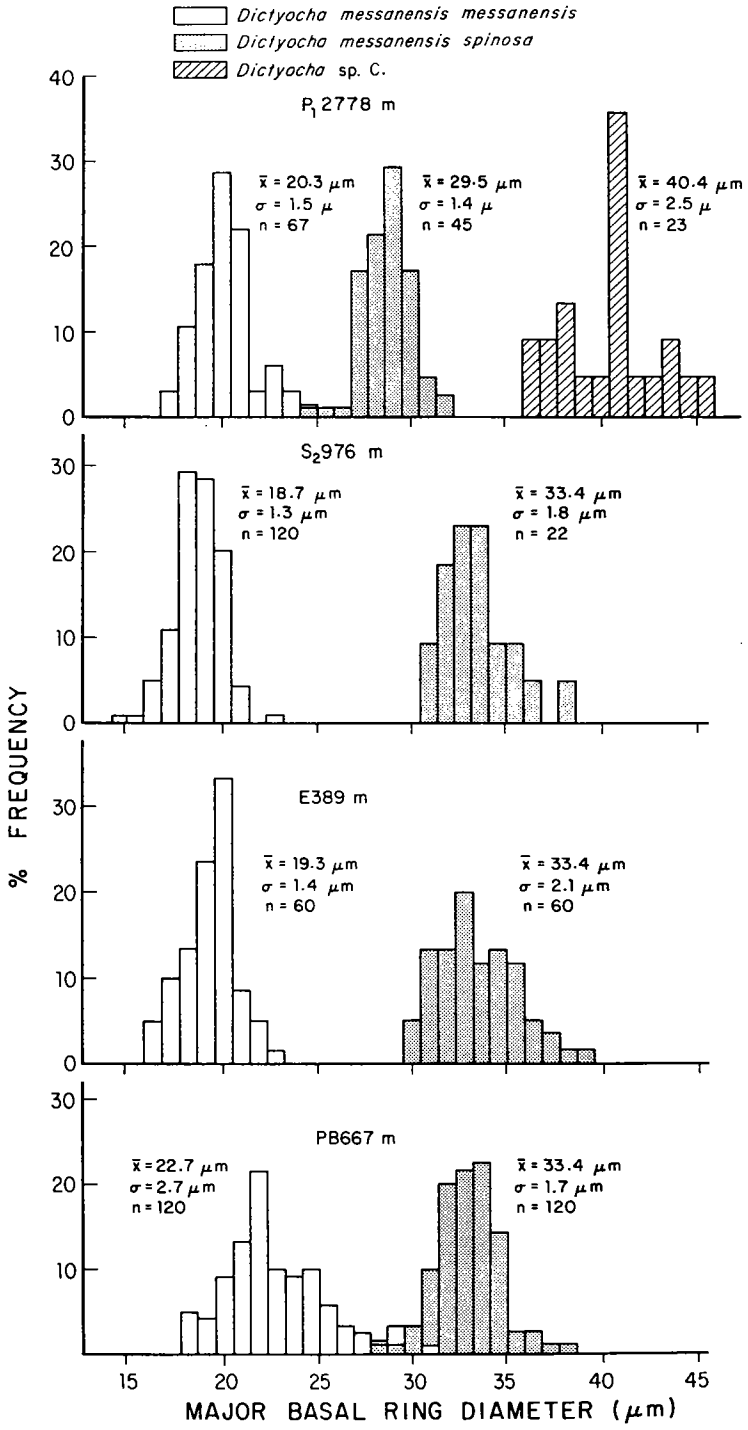

Figure 2: Histograms of major basal ring diameters for *Dictyocha messanensis messanensis*, *D. messanensis spinosa* and *Dictyocha* sp. C from four PARFLUX stations.

Table 4: Species fluxes (skeletons/m^2/day) of silicoflagellates and *Actiniscus* from PARFLUX sediment trap stations. Actual counts in each size fraction are given in Table 3. Numbers in parenthesis represent data corrected assuming spumellarian radiolarian flux was constant with depth (see text for details).

Station: and Depth (m)	*Dictyocha messanensis spinosa*	*Dictyocha messanensis spinosa* var. *pentagona*	*Dictyocha messanensis messanensis*	*Dictyocha mandrai*	*Dictyocha perlaevis*	*Dictyocha calida*	*Disthephanus pulchra*	Total Silicoflagellates	*Actiniscus pentasterias*
E: 389	61,416	0	30,056	794	0	0	35	92,301	—
988	49,174	0	52,825	1,432	0	0	163	103,594	—
3,755	100,448	0	108,822	1,966	0	0	246	211,482	—
5,068	56,393	0	91,639	1,896	0	0	137	150,065	—
P_1: 378	0	0	803	0	0	0	328	1,131	50
			(19,346)				(7,902)	(27,249)	(1,205)
978	89	0	7,831	0	0	0	2,792	10,712	131
	(300)		(26,401)				(9,413)	(36,114)	(442)
2,778	419	0	29,637	0	0	0	1,189	31,572	678
4,280	1,485	0	42,364	11	0	0	6,071	49,931	1,757
5,582	1,181	0	24,739	0	0	0	4,119	30,039	638
PB_1: 667	92,684	24	206,061	9,850	841	88,648	476,379	874,487	15,781
1,268	34,042	0	55,796	2,993	268	34,474	154,954	282,527	7,321
2,869	28,233	0	65,744	2,993	256	37,918	205,921	341,065	18,487
3,769	36,595	0	37,938	1,365	0	54,467	166,157	296,522	22,675
3,791	31,348	85	86,637	0	109	47,152	160,658	325,989	9,277

Dictyocha messanensis messanensis HAECKEL
Plate 1, figures 1, 5–6

Dictyocha messanensis forma *messanensis* Haeckel. POELCHAU, 1976, p. 173, pl. 1, figs. a, b; pl. 5, figs, a, c, d.

Dictyocha messanensis Haeckel. MURRAY AND SCHRADER, 1983, pl. I, figs. 14–18 (partim).

Dictyocha stapedia stapedia Haeckel. BUKRY, 1976, p. 724, pl. 3, figs. 1–7; 1980, p. 553, pl. 5, figs. 8–10.

DESCRIPTION: Basal ring rhombic, longitudinally elongate, with radial spines less than one half length of basal ring diameter. The radial spines at two polar positions are always longer than those at equatorial positions. Apical bar aligned in longitudinal position, about 1/3 of major basal ring diameter, and convex with an apical spine. Surface smooth.

DIMENSIONS: Major basal ring diameter 15–29 μm (Figure 2).

REMARKS: The specimens studied here are conformable with *D. stapedia stapedia* illustrated by Bukry (1976, 1980). The present specimens are smaller than *D. stapedia* in

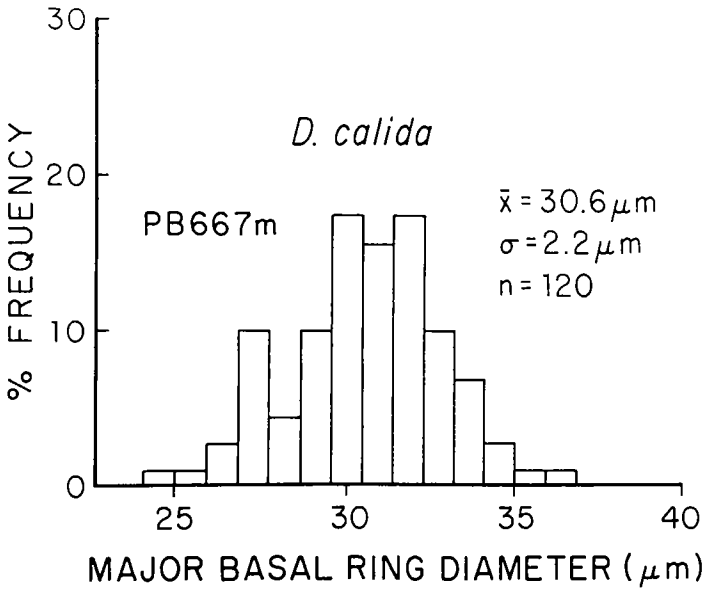

Figure 3: A histogram of the major basal ring diameter for *Dictyocha calida* from Station PB, 667 m.

Haeckel's (1887) original illustrations (31 μm in major basal ring diameter). A gradual reduction in size of this species has been observed in the geologic record (Bukry, pers. comm., 1983). From present-day oceans, based on trap material collected from a variety of locations and seasons, a significant size difference has been observed between stations (see text for a discussion on this subject). Several specimens illustrated as *D. messanensis* by Murray and Schrader (1983) are the same as the present taxon, and their size corresponds to that of the latter.

Dictyocha calida POELCHAU
Plate 1, figures 12 and 13

Dictyocha calida POELCHAU, 1976, p. 169, pl. 1, figs. c, d; pl. 3, figs. a–f. MURRAY AND SCHRADER, 1983, pl. II, figs. 14, 15.

Dictyocha calida calida Poelchau. BUKRY, 1980, p. 532, pl. 2, fig. 3.

Dictyocha calida ampliata BUKRY, 1980, p. 552, pl. 2, figs. 6–8.

DESCRIPTION: Basal ring is rhombic to square with gently curved basal bars of convex shape. Radial spines are 1/3 to 1/2 of basal ring diameter with polar and equatorial ones equal in length. Supporting spines located at the basal ends of apical rods. Apical bar is about 1/3 length of major basal ring diameter and always lies straight longitudinally. No apical spine. Convex shape of apical part is reduced for some specimens and therefore the whole skeleton becomes flat.

DIMENSIONS: Major basal ring diameter 24–32 μm (Figure 3).

REMARKS: This species' size distribution is similar to that of *D. messanensis spinosa*, but distinction between the two species is not difficult because of different morphology. Although this species was not found in Station P_1 trap samples, it was observed in a previous study of the Niskin bottle samples collected near Station P_1, but its abundance was low.

Dictyocha mandrai LING
Plate 1, figures 8–11; Plate 2, figure 1

Dictyocha fibula var. *aculeata* LEMMERMANN, 1901, p. 261, pl. 11, figs. 1, 2. LING, 1970, p. 91, pl. 18, figs. 11–13.

Dictyocha aculeata (Lemmermann). DUMITRICA, 1972, p. 907, pl. 9, figs. 5–10 (partim).

Dictyocha epiodon Ehrenberg. POELCHAU, 1976, p. 170, pl. 1, figs. e, f; pl. 4, figs. a–d. MURRAY AND SCHRADER, 1983, pl. I, figs. 7–12.

Dictyocha mandrai LING, 1977, p. 209, pl. 1, figs. 13, 14.

Dictyocha aculeata aculeata (Lemmermann). BUKRY, 1980, p. 549, pl. 1, figs. 1–3.

See Ling (1970, 1977) and Dumitrica (1972) for more synonymies.

DESCRIPTION: Basal ring is rhombic to octagonal and elements of basal rings convex, with subordinate short conical radial spines alternating with major radial spines. Supporting spines are longer than those of *D. messanensis* and very conspicuous because of their size, which is one of the major characteristics of this species. The axis of apical bar at two poles is offset from that of radial spines by about minus 12° (8–16°). Length of the apical bridge is about 1/3 of major basal ring diameter. Apical spine present. Surface smooth, with or without many micro-spines.

DIMENSIONS: Major basal ring diameter ranges from 26 μm to 55 μm and there is a discontinuity between small and large forms (see Figure 4).

REMARKS: Size measurements indicate that there is a definite bimodal distribution of this species at Station S_2. Only the small form was encountered at stations P_1 and PB. Both forms were observed at Station E, but the larger form predominated. This species has been also referred to as *D. aculeata* and *D. epiodon* by some workers. See Ling (1977) for a discussion regarding the name of this species.

Dictyocha perlaevis FRENGUELLI
Plate 2, figures 2–4

Dictyocha perlaevis FRENGUELLI, 1951, p. 279, figs. 4b, c. (*fide* LOEBLICH et al., 1968, p. 40, 109, pl. 51, figs. 7, 8). DUMITRICA, 1973a, p. 848, pl. 3, figs. 8–12; pl. 4, figs. 1, 2.

Dictyocha perlaevis perlaevis Frenguelli. BUKRY, 1980, p. 553, pl. 4, figs. 3–9; pl. 5, figs. 1–3.

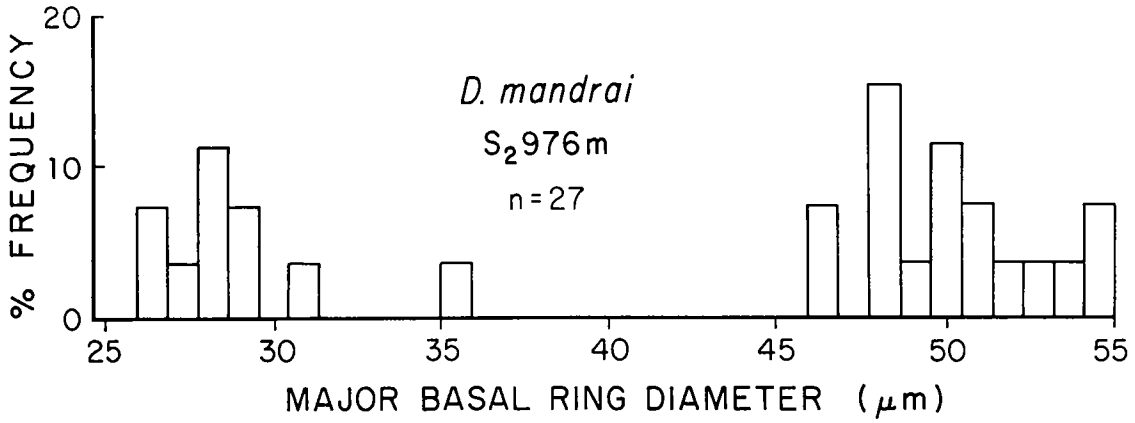

Figure 4: Histograms of the major basal ring diameter for *Dictyocha mandrai* from Station S_2, 976 m.

DESCRIPTION: Basal ring is large, rhombic, longitudinally elongate, with elements of basal ring convex, radial spines short. Axis of apical bar is slightly offset from that of two polar spines and its length is about 1/3 of major basal ring diameter. Normally, longitudinal length of the basal ring is only slightly greater than its width, but for some specimens the minor basal ring diameter is reduced up to 60% of major basal ring diameter, causing an elongate basal ring.

DIMENSIONS: Major basal ring diameter 57–69 μm. Minor basal ring diameter 50–57 μm.

REMARKS: The skeletal dimensions of this taxon are two to three times larger than the other taxa encountered. The size is one of the most distinguishing criteria which separates this species from the rest of the taxa. Continuous transition from square form to elongate form exists, but whether this constitutes normal distribution (or bimodal or polymodal) is not known due to scarcity of specimens. This species was found only at Station PB. All of the specimens examined here were about 60 μm in major basal ring diameter. Small forms, about 40 μm illustrated by Bukry (1980), were not encountered here. Two specimens bearing rectangular apical rings (Plate 2, figure 2) have been found and tentatively assigned to this species.

Genus *Distephanus* (Stöhr) HAECKEL

Distephanus pulchra (Schiller) LING AND TAKAHASHI
Plate 2, figures 5–11

Mesocena octogona EHRENBERG, 1843 (*fide* Loeblich et al., 1968, p. 129, pl. 27, fig. 6); *Mesocena heptagona* EHRENBERG, 1843 (*fide* Loeblich et al., 1968, p. 128, pl. 27, fig. 5).

Distephanus octogonus (Ehrenberg). DUMITRICA, 1972, p. 908, pl. 12, figs. 15–19.

Distephanus octonarius Deflandre. LING, 1973, p. 752, pl. 2, figs. 5, 6; 1977, p. 207, pl. 2, fig. 11.

Octactis pulchra Schiller. BUKRY AND FOSTER, 1973, pl. 6, figs. 11, 12. POELCHAU, 1976, p. 177, pl. 6, figs, h–j. BUKRY, 1980, p. 553, pl. 8, figs. 11, 12. MURRAY AND SCHRADER, 1983, pl. I, figs. 1–6.

Distephanus pulchra (Schiller). LING AND TAKAHASHI, 1985, pl. 1, figs. 4–9; pl. 2, figs. 1–4, 7.

See Dumitrica (1972) and Ling and Takahashi (1985) for more complete synonymies.

DESCRIPTION: Basal ring usually octagonal and occasionally nine- to ten-sided polygonal, frequently slightly elongated, with eight to ten slender conical radial spines whose lengths range from 1/3 to 1/2 of major basal ring diameter. Commonly, the radial spines on the two polar points are the longest of all. Apical ring is octagonal to circular, its diameter is slightly less than that of basal ring, and has a delicate skeleton which tends to collapse easily. Apical spines are very short, conical, often not recognizable perhaps due to dissolution. No supporting spines. Skeletal surface is smooth.

DIMENSIONS: Major basal ring diameter 17–28 μm. Radial spine length 6–14 μm. Apical ring diameter 64–90% of basal ring diameter.

REMARKS: Species name proposed by Ling and Takahashi (1985) is used here and the reader is referred to their discussions regarding the assignment of species name. This is the most abundant taxon at Station PB whose flux at 667 m reaches nearly half a million skeletons/m^2/day. Based on major basal ring diameter measurements, two populations may be present at Station P_1 (Figure 5); one centered at 21 μm size and the other at 24 μm size in basal ring diameter.

Class DINOPHYCEAE
Order GYMNODINIDA
Family ACTINISCIAE KÜTZING
Genus *Actiniscus* EHRENBERG, 1854

Actiniscus pentasterias (Ehrenberg) EHRENBERG
Plate 2, figures 12–15

Dictyocha (Actiniscus) pentasterias EHRENBERG, 1841, pp. 111, 149.

Actiniscus pentasterias (Ehrenberg). EHRENBERG, 1854, pl. 18, fig. 61; pl. 19, fig. 45; pl. 20, fig. 48; pl. 33, fig. 1; pl. 35A, fig. 1; pl. 36, fig. 36. DUMITRICA, 1973b, p. 822, pl. 2, figs. 2, 3, 6–11, 14; pl. 3, figs. 13, 14; pl. 5, figs. 6–8. ORR AND CONLEY, 1976, p. 92, pl. 1, figs. 1–11; pl. 2, figs. 1–6. PERCH-NIELSEN, 1978, p. 154, pl. 5, figs. 1–7, 9–11; pl. 6, figs. 9, 13–16.

See Dumitrica (1973b) for a more complete synonymy.

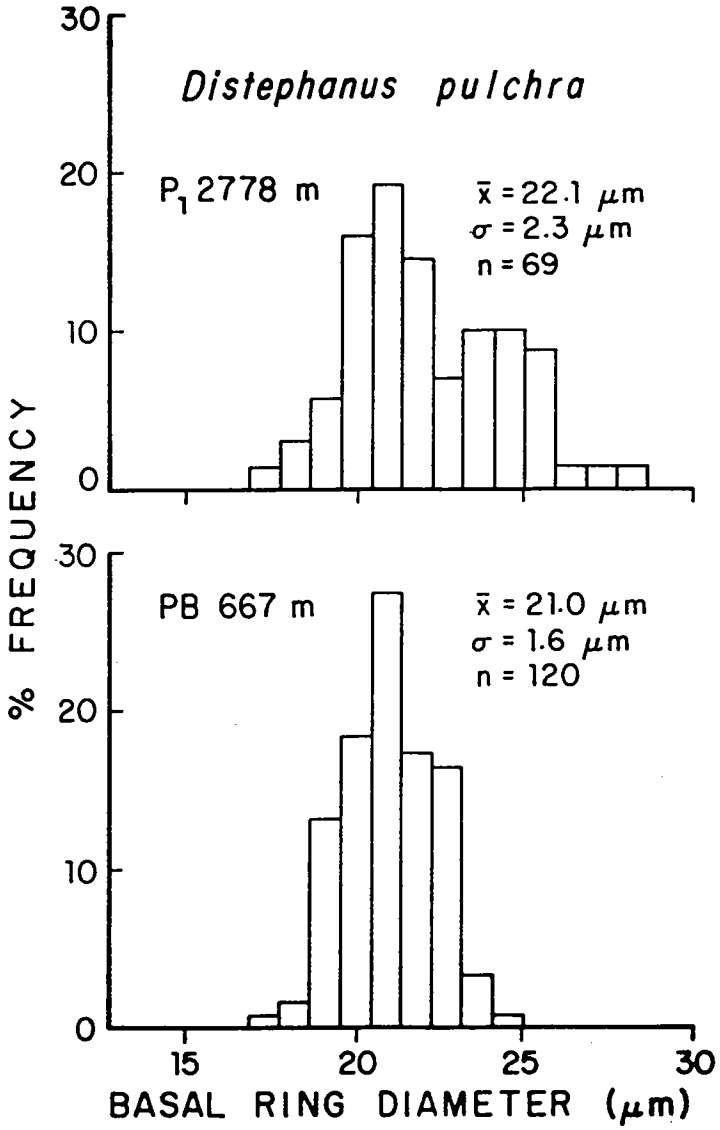

Figure 5: Histograms of the basal ring diameter for *Distephanus pulchra* from Stations P_1, 2,778 m and PB, 667 m. Note that the Station P_1, 2,778 m sample presents bimodal distribution and its secondary peak around 24 μm is absent in Station PB, 667 m data.

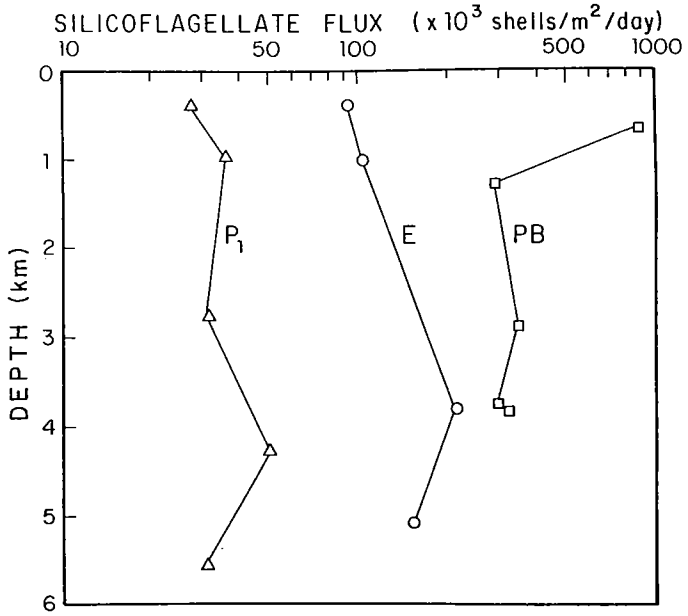

Figure 6: Total silicoflagellate species fluxes at three PARFLUX stations. Data from Station P_1, 378 m, and P_1, 978 m, were corrected using spumellarian radiolarian flux assuming that true spumellarian flux did not change from epipelagic to bathypelagic zones.

DIMENSIONS: Maximum diameter between two arms 18–35 μm. Mean, standard deviation and number of specimens for the maximum diameter are: Station P_1, X = 21.9 μm, σ = 2.1 μm, n = 12; Station PB, X = 27.6 μm. σ = 3.7 μm, n = 15; Station E, X = 22.5 μm, σ = 0.7 μm, n = 2.

REMARKS: This is the only dinoflagellate species bearing siliceous endoskeleton found in the present study. Wide variation in size has been observed. Also, skeletal surface texture can be variable (compare Plate 2, figures 12 and 14). The flux of this species is rather small and never exceeded 8% of total silicoflagellate flux (skeleton number) values.

Results and Discussions

Silicoflagellate Fluxes

Vertical fluxes (skeletons/m^2/day) of total silicoflagellates at three PARFLUX stations are illustrated in Figure 6. Data from Station P_1, at 378 m and 988 m, were corrected using the flux of spumellarian radiolarians, assuming that spumellarian flux was uniform throughout the water column at this station. Another assumption made in the correction is that the silicoflagellate/spumellarian ratio remained the same in the mesopelagic zone as in the bathypelagic zone. Particle fluxes, including spumellarians, at these two depths appear to be affected by "swimmers". The present concensus (e.g., Honjo, 1980) is that the smaller fluxes at these two depths were probably due to incidental visitors such as macrozooplankton and small nektons. These "swimmers" may cause a serious error in biogenic

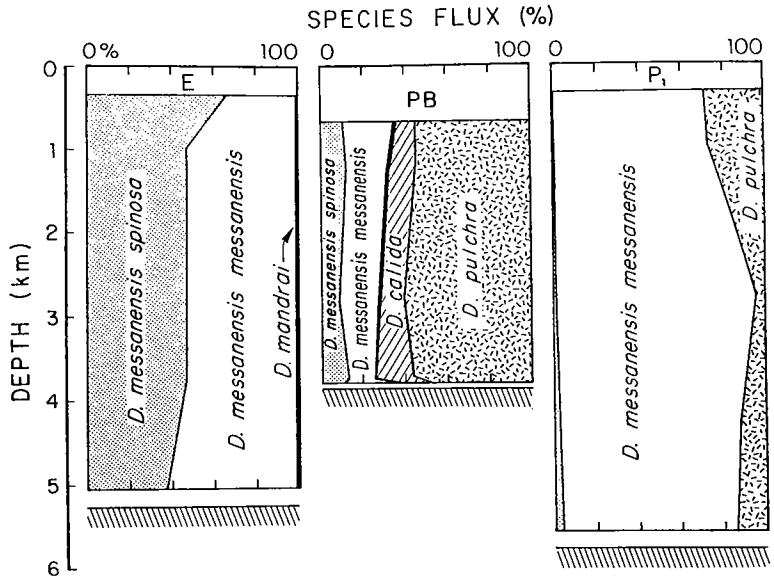

Figure 7: Percent silicoflagellate fluxes at three PARFLUX stations.

flux assessment of sediment trap material, especially for trap material collected in shallow waters where zooplankton are active (Honjo, 1980). Polycystine Radiolaria, particularly Spumellaria, have shown to give constant fluxes throughout pelagic environments since the dissolution effect during their settling time span is not enough to cause faunal assemblage change (Takahashi, 1981). Therefore, an attempt was made to normalize silicoflagellate fluxes at the top two depths using spumellarian average fluxes from the bathypelagic zone.

Total silicoflagellate flux at Station P_1, southeast of Hawaii, was relatively uniform throughout the trap depths, considering a 25% accuracy error of analysis. *Dictyocha messanensis messanensis* constituted 71 to 94% of the flux depending on depth at this station and thus was the predominant taxon (Figure 7) during the trap experiment. The relative flux abundance of this taxon is followed by *Distephanus pulchra* (4 to 29%). *Dictyocha calida* was not encountered in this study, although its presence is known in areas just to the south (Poelchau, 1976, stations SCAN 654, MSN 143PG) and east (Takahashi, unpublished data, DOMES stations B, C).

The flux at Station E, in the tropical North Atlantic, increased by a factor of two from mesopelagic to middle bathypelagic zones and then slightly decreased toward the bottom (Figure 6). The maximum flux at Station E, 3,755 m, was also noticed in other studies including the radiolarian paper in the Ocean Biocoenosis Series (Takahashi, in press). When this flux curve is compared with a group of curves for the *D. messanensis spinosa*/*D. messanensis messanensis* ratio (Figure 8b), whose details are discussed below, they correspond inversely suggesting that there is a close negative correlation between the two; as the flux increases, the ratio of *D. messanensis spinosa*/*D. messanensis messanensis* decreases. This negative correlation may well be an indication of seasonality during the 98-day deployment. A radiolarian study at this station did not indicate such a seasonal trend throughout the depths (Takahashi and Honjo, 1981). The majority of silicoflagellates, at least at Station E, settle initially in the form of aggregates in the mesopelagic zone, and then some of them

gradually disintegrate in the bathypelagic zone (Figure 8) and are subjected to dissolution. Therefore, we would expect a decrease of flux with depth if the supply was constant through time. The twofold increase of the flux from mesopelagic to bathypelagic zones implies a greater amount of initial input for the 3,755 m sample than that at shallower depths.

Individually settling silicoflagellates which sink at a rate of about 1.4 m/day (see below for discussion) are not expected to contribute significantly to the vertical flux because they should be dissolved in less than 1 km vertical distance. Therefore, in order to account for observed fluxes it is necessary to invoke relatively fast or dissolution-protected modes of sinking such as in aggregate form or in marine snow.

The two subspecies of *D. messanensis* were easily distinguished by their distinctively different sizes; *D. messanensis spinosa* is 45 to 79% larger in major basal ring diameter than *D. messanensis messanensis* (Figure 2). Other differences between the two subspecies are angle of apical bar tilt from the major axis, length of apical bar, and ratio between major and minor basal ring diameter (see Plate 1, figures 1–6). The *D. messanensis spinosa*/*D. messanensis messanensis* ratio generally decreased with depth. This supports the concept that individual settling silicoflagellates are not a major factor in sedimentation. *D. messanensis spinosa* is larger and more robust than *D. messanensis messanensis* and therefore one would expect better preservation of the former than the latter, if individual sinking is taking place. However, the fact that the flux of *D. messanensis messanensis* increases with depth suggests that such individual sinking is unlikely.

Since the best sample preservation occurred in Station E material, the original sample configuration has been retained better than in other samples. As a result, a percentage of silicoflagellate skeletons in biogenically processed aggregates, analogous to the radiolarian study (Takahashi and Honjo, 1981), was obtained (Figure 8a). One half of the skeletons were in the form of aggregates, possibly processed by animals, suggesting that predation may be an important process in packaging silicoflagellates into the aggregates and in transforming the sinking mode from slow to fast. Also, number of silicoflagellate skeletons associated with aggregates in the samples (250–125 μm) from Station S_2, 976 m, was 54%. Other workers also found silicoflagellates in fecal pellets (e.g., Honjo, 1978, 1980; Dunbar and Berger, 1981) (although the fecal pellet association may be a minor contribution to deep-sea sedimentation) and in marine snow (Silver and Alldredge, 1981). As depth increases the percentage of silicoflagellates decreases to about 25% for at least two size fractions, suggesting that disintegration en route may have occurred. Data from 63–125 μm size fraction present a somewhat deviated trend from the rest. Since this size fraction represents small fragments of aggregates, it is more easily disintegrated than the larger size fractions. Therefore, size fractions 125–250 μm and 250–1000 μm provide better information than the 63–125 μm size fraction.

The decrease of percentage of silicoflagellates in aggregates with depth is contrary to the flux increase at 3,755 m because disintegration will cause the skeletons to be freed and to settle individually. Since the individual settling of silicoflagellates is so slow, approximately 1.4 m/day in deep sea conditions (Poelchau, 1974, original data are about 2.7 m/day but reduced by 42% here after examination of his methods as discussed in a later section), it would not contribute much to the flux because of dissolution. Therefore, the percent and flux data support the idea of there being different amounts of silicoflagellates in the source

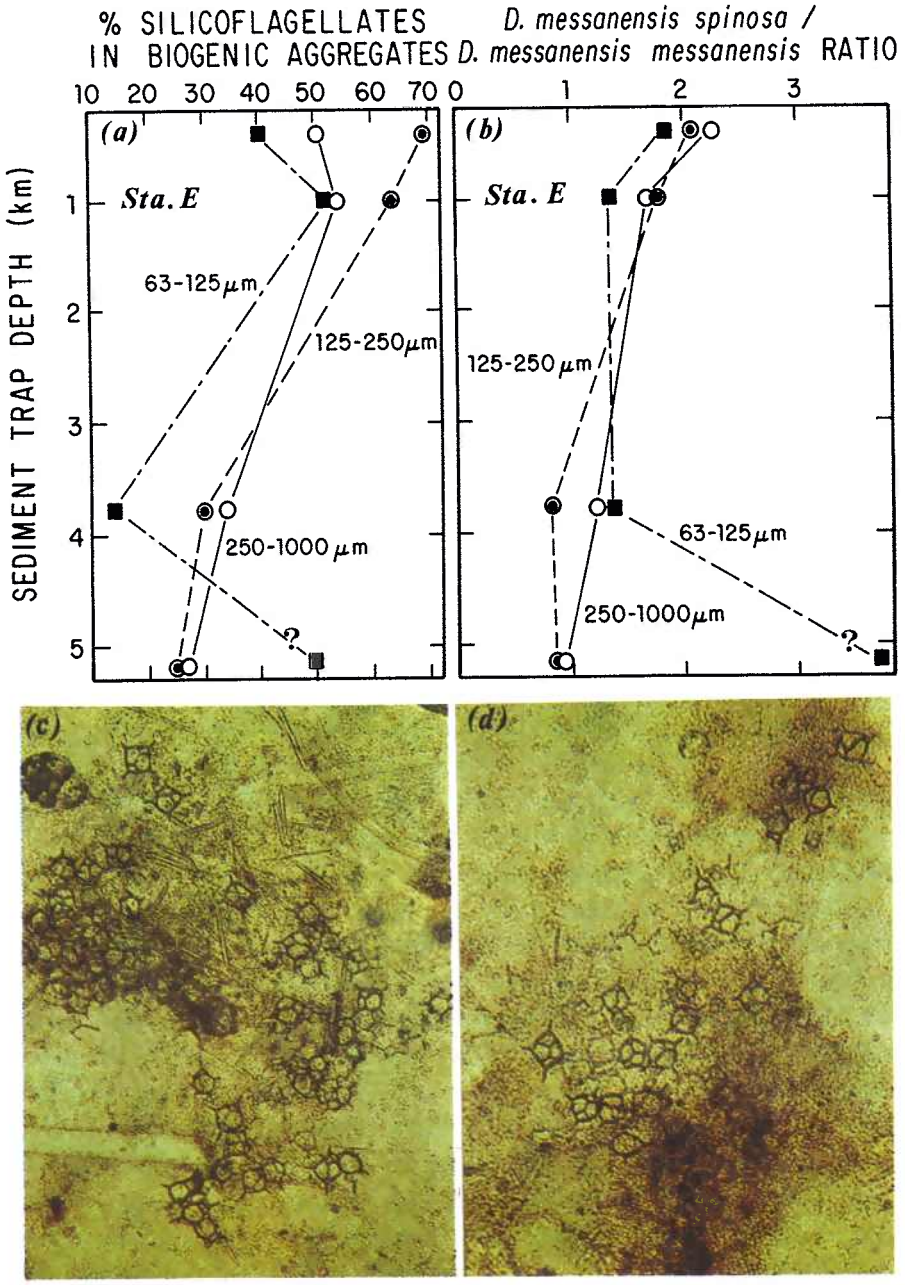

Figure 8: (a) Percentage of silicoflagellates transported in aggregated particles at Station E. (b) *Dictyocha messanensis spinosa*/*D. messanensis messanensis* ratio at Station E. Note a trend in decrease of percent aggregates and ratio with increasing depth. (c, d) Photomicrographs showing silicoflagellates associated with organic aggregates; Station E, 389 m, × 110 for both. Note that abundant spines of *Sticholonche zanclea* (Heliozoa) are also associated within the aggregate (c).

zone, which indicates seasonality in production or other factors such as a different levels of predation.

The results from the Panama Basin Station show a different kind of silicoflagellate flux than the other stations. Here, the flux decreased by 64% from the mesopelagic to upper bathypelagic zone and then remained uniform below (Figure 6). Possibly one type of aggregate containing silicoflagellates disintegrated prior to arrival at the upper bathypelagic zone but the other type was more resistant to breakage and hence arrived at the bottom without distruction. Seasonality is an alternative explanation but is unlikely because the species' composition did not change much throughout the water column (Figure 7).

Although there is no quantitative count of silicoflagellate flux at Station S_2, 3,694 m, microscopic examinations indicated that the difference in flux was not more than a factor of three from that found at 976 m, if not equal. An analysis of 10 grams (wet) of the surficial bottom sediments taken by a box core at Station S_2 and wet sieved with 20 μm mesh revealed a total absence of silicoflagellates, suggesting that all of the silicoflagellate supply is dissolved on or near the sea floor.

Silicoflagellate fluxes were largest at Station PB, followed by Stations E and P_1 (Table 5). The same trend has been found in the radiolarian flux (Takahashi, in press) and foraminiferal flux (Thunell and Honjo, 1981; Thunell et al., 1983). The silicoflagellate flux followed general productivity regimes: from the hemipelagic, relatively eutrophic Panama Basin to an intermediate productive Station E in the western Atlantic, and then to the oligotrophic Station P_1 at the margin of the North Pacific central gyre.

A positive correlation between radiolarian and silicoflagellate fluxes is apparent (Figure 9): a coefficient of r=0.92 was obtained when an anomalous value at PB 667 m was excluded (r=0.76 when it was included). Correlations between either silicoflagellate or radiolarian flux and calcareous plankton groups (coccolithophores, coccoliths and foraminifera) showed that although correlations are generally positive, the coefficients are smaller than the above correlation between the two siliceous groups. For instance, a correlation coefficient between silicoflagellate and foraminiferal fluxes is r=0.57.

As noted earlier, the percentage of *D. messanensis messanensis* in silicoflagellate flux was higher at Station P_1 than at Station PB. Organic carbon fluxes (Honjo et al., 1982) were compared to the relative abundance of *D. messanensis messanensis* (Table 5; Figure 10). We note a clear trend of this taxon as an oligotrophic water indicator based on the data from the four trap stations. Similar evidence was present based on plankton assemblages of silicoflagellates collected from the Gulf of California (Murray and Schrader, 1983). On the other hand, the flux of *D. pulchra* appeared to increase as organic carbon flux increased (Figure 10). Thus, *D. pulchra* is a fertility indicator as proposed in an independant study by Murray and Schrader (1983).

The silicoflagellates recovered from abyssal zones must have been vertically transported by some sort of fast sinking mode rather than by slow individual sinking. The dissolution effect on individual skeletons during such a long journey (more than a year to sink 1 km vertical distance) is enough to eliminate them from the water (Hurd and Birdwhistell, 1983). As demonstrated clearly by an example from Station E, organic aggregates are the major transporting mechanism of silicoflagellates in certain environments. Although the exact sinking rates are not known, silicoflagellates in aggregates may sink fast enough to

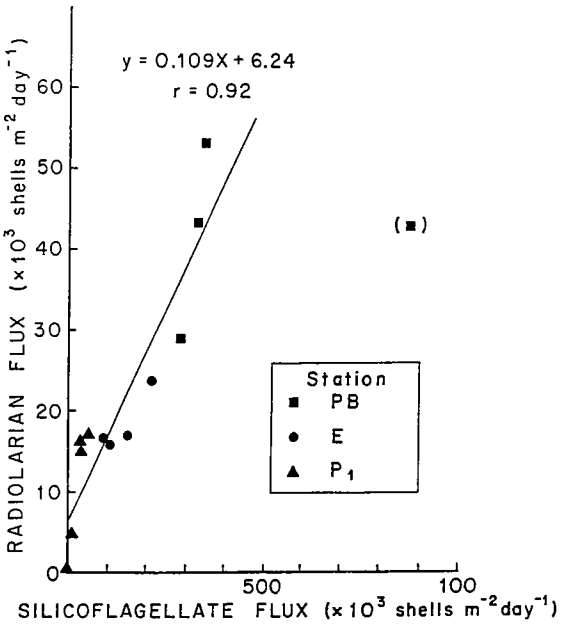

Figure 9: Plots of silicoflagellate flux vs. radiolarian flux from three PARFLUX low latitude stations. An anomalous datum point from Station PB 667 m was excluded from the regression line drawn here.

eliminate different seasonal signals observed in the different trap depths at stations P_1 and PB but slow enough to show the seasonality observed at Station E. Also, other aggregates such as marine snow are important transport mechanisms for silicoflagellates (Silver and Alldredge, 1981).

Occurrences of slightly abnormal skeletons such as five-sided *D. messanensis* (Plate 1, figure 15) or *D. mandrai* (Plate 2, figure 1) were quite rare in the course of the present study (Table 4). Other than the octagonal *D. pulchra*, nine- and ten-sided specimens occurred frequently. Furthermore, no cold water form (e.g., *Distephanus speculum*) was found during the census (in more than 30 thousand specimens). Silicoflagellates in the laboratory and in stressed environments such as brackish water, however, are known to produce irregular skeletons of *Dictyocha* species (Shitanaka, 1983). It appears that silicoflagellate skeletal morphology is conserved consistently in tropical pelagic environments.

Actiniscus Fluxes

Fluxes of *Actiniscus pentasterias* were small compared to those of total silicoflagellates (1 to 4% and 2 to 8% at stations P_1 and PB, respectively). Large variations of their flux values was observed at both stations (P_1 and PB), due to small sample size. No consistent trend of decreasing or increasing of fluxes with depth was found. Their mode of sedimentation may well be similar to those of silicoflagellates; the major means of vertical transport, therefore, is assumed to be settling with oceanic aggregates.

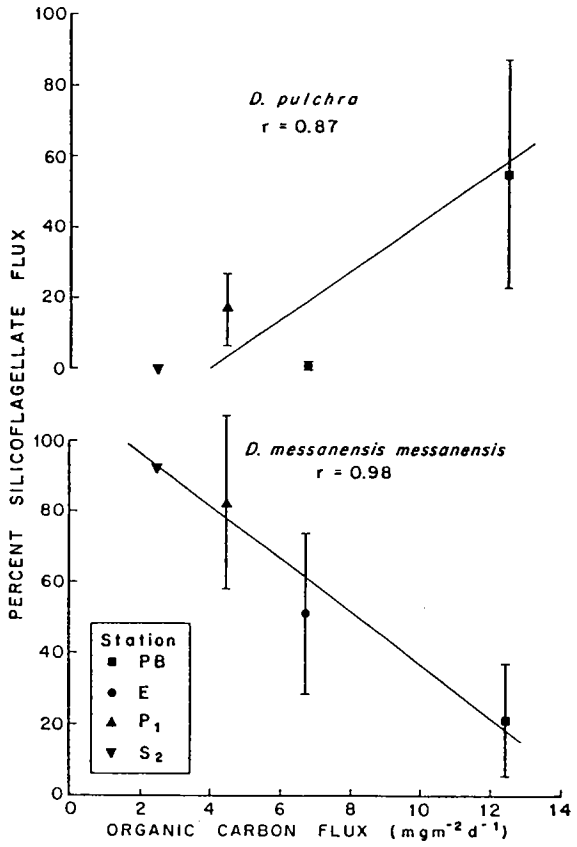

Figure 10: Plots of organic carbon flux (from Honjo et al., 1982) vs. flux percentage of silicoflagellate taxa. *Distephanus pulchra* may indicate fertility and *Dictyocha messanensis messanenesis* may indicate oligotrophic water.

SiO_2 Mass Flux Due to Silicoflagellate Skeletons

In order to assess the percent contribution of silicoflagellates to total opal flux, individual skeletal mass must be known. Lisitzin (1971) speculated that the average skeletal weight ratio between siliceous organisms was, silicoflagellate:diatoms:radiolarians = 1:5:250. The ratio between silicoflagellates and diatoms was merely derived on the basis of visual observations of their skeletons and thus it may be far from the true value. The weight of a silicoflagellate skeleton is estimated to be from 0.004 to 0.012 μg (4 to 12 ng) (Lisitzin, 1971). The value 0.004 μg/skeleton can be multiplied by total silicoflagellate flux values and then compared with total opal SiO_2 values from each station (Honjo et al., 1982). The following are the estimated minimum percent contributions of silicoflagellate to total biogenic opal flux in the abyssal zone: P_1, 6%; E, 14%; and PB, 4%. Judging from microscopic observations of the trap material as well as knowledge of measurements of thousands of radiolarian skeletal weights (Takahashi and Honjo, 1983), these percentages are too high, probably by a factor of three to four. For instance, the radiolarian contribution to total opal flux at Station PB was estimated, based on weights and counts, to be from 22 to 30%

depending on depth (Takahashi, 1981). A volume computation of silicoflagellate skeletons based on SEM micrographs combined with counts showed that silicoflagellates could not contribute more than a few percent of radiolarian opal flux at Station PB.

In the absence of desirable data, at best, an empirical equation for predicting radiolarian sinking speed using weight, or *vice versa*, can be used to estimate the weight of a silicoflagellate: log [sinking speed] (m/day) = 0.5 log [weight (μm)] + 1.88 (Takahashi and Honjo, 1983). Poelchau (1974) measured average sinking speeds of silicoflagellates at 2.7 m/day in distilled water at 24°C, using a method similar to that of Berger and Piper (1972). In order to make this datum comparable to the radiolarian sinking speed data which were obtained in seawater (salinity = 36.1°/$_{oo}$) at 3°C, a conversion factor of 0.520 (Berger and Piper, 1972) was applied; thus Poelchau's sinking speed was modified to 1.4 m/day and the skeletal weight was extrapolated as 0.34 ng/shell. Using a weight of 0.34 ng/shell, the following is the percent of the total biogenic opal flux due to silicoflagellates at each station: P_1, 0.5%; E, 1.2%; PB, 0.3%.

Silicoflagellate Preservation in Holocene Sediments in Relation to Supply

Honjo (unpublished data) has estimated a net sedimentation rate of 0.45 mg/m^2/day at Station P_1, which can be extrapolated to 16.425 mg/cm^2/10^3/yr. Total silicoflagellate flux at the deepest trap (5,582 m) at Station P_1 was approximately 30 $\times$ 10^3 skeletons m^2/day or 1095 $\times$ 10^3 skeletons/cm^2/10^3/yr. According to Poelchau (1974), one gram of surface dry sediment at an area near the station contained 10 $\times$ 10^3 skeletons. Using Honjo's value given above, this would have taken 60.79 $\times$ 10^3 years to accumulate, and thus the estimated silicoflagellate accumulation rate is 0.1645 skeletons/cm^2/10^3/yr. This value is 0.015% of the total silicoflagellate flux value. When Kozlova and Mukhina's (1967) values of 30–420 $\times$ 10^3 skeletons/g is used, a maximum of 0.63% preservation is obtained with similar calculations. Therefore, in the vicinity of Station P_1 less than one percent of the silicoflagellate flux has been preserved on the sea floor. Poelchau (1974), on the other hand, arrived at a figure of 3% preservation, using different types of data and assumptions. It is clear that the majority of silicoflagellates are dissolved on the sea floor in the area of Station P_1. Despite the relatively large flux at Station S_2, no silicoflagellate skeletons are preserved in the surficial bottom sediments, indicating total dissolution at the water-sediment interface.

Size of Silicoflagellate Skeletons

In order to study skeletal size variability of different populations, the diameter of the basal ring in the major axis (major basal ring diameter) was chosen as a criterion. Samples collected from the topmost trap depth were used to measure the major basal ring diameter at three stations. At Station P_1, samples which were concentrated enough to study were available only at 2,778 m depth and below.

Of the populations from any pair of the four stations, *D. messanensis messanensis* was the only taxon to show significant differences in skeletal size in *t* tests (Table 6). In general, the higher the temperature the larger the skeleton size of this taxon. The temperature range above the thermocline and average depth of the bottom of the thermocline

Table 5: Mean flux (No. $m^{-2}d^{-1}$) and percentage (in parentheses) of silicoflagellate taxa. Organic carbon flux data from the tops of mesopelagic zones are taken from Honjo et al. (1983).

Station	Organic C ($mg\ m^{-2}d^{-1}$)	*Dictyocha messanensis spinosa*	*Dictyocha messanensis messanensis*	*Dictyocha mandrai*	*Dictyocha perlaevis*	*Dictyocha calida*	*Disthephanus pulchra*	Total Silicoflagellates
PB_1	12.55	44,580 (10.5%)	90,435 (21.3%)	3,440 (0.8%)	295 (0.1%)	52,532 (12.4%)	232,814 54.9%)	424,118 (100.0%)
E	6.73	66,858 (48.0%)	70,836 (50.8%)	1,522 (1.1%)	0	0	145 (0.1%)	139,361 (100.0%)
P_1	4.58	677 (1.9%)	28,497 (81.5%)	2	0	0	5,739 (16.4%)	34,981 (99.8%)
S_1	2.43	1,043[a] (5.9%)	16,136[a] (91.8%)	385[a] (2.2%)	0	0	0	17,576[a] (99.9%)

[a]Based only on 250–125 μm size fraction.

during trap deployments is as follows: S_2, 23–20°C, 100 m; P_1, 25–14°C, 130 m; E, 27–24°C, 100 m; PB, 27–19°C, 75 m. In detail, the data from stations P_1 and E did not follow this general size-temperature trend, but their sizes are so close ($z = 2.77$ in t test) that the size difference was marginally significant.

On the other hand, the major basal ring diameter of *D. messanensis spinosa* was similar between populations at stations S_2, E, and PB (Table 6). However, a population at Station P_1 showed very different sizes from the rest of the stations (Figure 2). Oligotrophic conditions at Station P_1 relative to the other stations may be responsible for the size difference. Poelchau (1976) showed such a size difference in this species from the eastern and western sides of the North Pacific.

A difference was noted between histograms of the Pacific and Atlantic populations of the above two taxa. While there is a continuity in size distribution of *D. messanensis messanensis* and *D. messanensis spinosa* at stations P_1 and PB (both Pacific), size distribution histograms of the two species at stations S_2 and E (both Atlantic) show them as distantly isolated (Figure 2).

Dictyocha mandrai shows two populations whose sizes are clearly separated (Figure 4). The shapes of the two populations are very similar to each other and therefore they were not distinguished during the census. Dumitrica (1972) previously had noticed a similar size difference in *D. mandrai* specimens from Quaternary Mediterranean sediments. Poelchau (1974) illustrated the size distribution of this taxon, taken from middle latitudes in the northwest Pacific, which ranged from 20 to 40 μm in basal ring diameter.

Table 6: The Z values for t tests between two stations for the major basal ring diameter of silicoflagellate species.

Station: **Depth (m)**	**P_1:** **2778**	**S_2:** **976**	**E:** **389**	**P_1:** **2778**	**S_2:** **976**	**E:** **389**	**P_1:** **2778**
	Dictyocha messanensis spinosa			*Dictyocha messanensis messanensis*			*Distephanus pulchra*
S_2: 976	8.93			7.33			–
E: 389	11.40	0		3.89	2.77		–
PB: 667	13.46	0.97	1.28	7.81	14.62	11.12	3.51

There may be two populations of *Distephanus pulchra* (Figure 5). Data from Station P_1 show bimodal distribution, and the secondary mode is absent in a histogram from Station P_1. The size of the primary mode is the same at the two stations. The majority of specimens bear very fragile apical rings, but some robust forms which are slightly larger than the fragile ones bear apical rings equally as thick as their basal rings and often they are more than eight sided (Plate 2, figure 10).

Summary

Silicoflagellate fluxes and species composition at Station P_1 did not fluctuate much throughout the water column, suggesting that the sample source, in terms of time span of silicoflagellate production, was the same for all the trap depths. This result is similar to that found in a radiolarian study. Station E, on the other hand, showed consistent change in species composition throughout the water column as well as an increase in flux with depth, suggesting a possible seasonality in the flux as measured from different trap depths. The number of silicoflagellate skeletons in aggregates was estimated to be about equal to that of discrete skeletons in the mesopelagic zone at Station E. The value decreased with increasing depth, suggesting disintegration of the organic matrix of the aggregates as they fall through the water column.

Station PB showed a 64% decrease in silicoflagellate flux from the mesopelagic to upper bathypelagic zone, but seasonality does not account for this flux change based on species composition data alone. The decrease is exponential and similar to that of organic carbon flux, suggesting that aggregate disintegration may be an important process in the resultant flux at Station PB. Uniform flux below the upper bathypelagic zone and similar species composition throughout suggests that fast sinking of the silicoflagellates via aggregates appears to be taking place.

The major site of silicoflagellate dissolution is on the sea floor. Although the postulated details of the processes are different, the present result conforms to the notion that the majority of silicoflagellate skeletons reach the sea floor without being dissolved (Kozlova and Mukhina, 1967).

The magnitude of silicoflagellate fluxes at three PARFLUX stations differs in accordance with regional primary productivity, and is in descending order: stations PB, E, and P_1. This flux rank at the three stations conforms with those of Radiolaria and Foraminifera. Four major species of silicoflagellate contribute the bulk of the flux at Station PB, while two major species at Station E and a single species at Station P_1 predominate in the assemblages. As nutrient conditions become more oligotrophic the diversity of dominant species decreases. Thus, silicoflagellates in fossil assemblages have a potential as a productivity indicator.

Mass balance calculations using flux and the skeletal weight of silicoflagellates suggest that they contribute one percent or less to biogenic opal flux at each station. The estimated weight of the skeleton is about 0.34 ng/shell which is one to two orders of magnitude less than that previously estimated by Lisitzin (1971).

Only less than one percent of silicoflagellate flux was estimated to be preserved in the Holocene sediments at Station P_1. No silicoflagellates were preserved in the surface sediments at Station S_2, suggesting total dissolution on the sea-floor.

Size distribution is a useful tool to separate two closely related taxa such as *D. messanensis messanensis* and *D. messanensis spinosa*. A significant size difference in a single taxon was often found between stations; some differences are correlated with temperature and/or nutrients.

Acknowledgments

Dr. Susumu Honjo at Woods Hole Oceanographic Institution has conducted all phases of the PARFLUX sediment trap project from which all samples used in this study were obtained. His enthusiastic encouragement and discussions throughout the course of the investigation not only sustained but also greatly enriched this chapter. The manuscript has been critically and constructively reviewed by Drs. S. Honjo, H.Y. Ling, D. Bukry, and R. Thunell. This work was supported by NSF grants OCE-8019386 and OCE-8208638. The samples used in this research were collected during the 1976 to 1979 PARFLUX experiments and the 1979 Sediment Trap Intercomparison Experiment which were supported by NSF grants OCE-7682063, OCE-7727004, and OCE-7925429.

References

Berger, W.H. and D.J.W. Piper (1972). Planktonic foraminifera: differential settling, dissolution and redeposition. *Limnol. Oceanogr.*, **17**:275–286.

Brewer, P.G., Y. Nozaki, D.W. Spencer and A.P. Fleer (1980). A sediment trap experiment in the deep subtropical Atlantic: isotopic and elemental fluxes. *Jour. Mar. Res.*, **38**(4):703–728.

Bruland, K.W., R.P. Franks, W.M. Landing and A. Soutar (1981). Southern California inner basin sediment trap calibration. *Earth Planet. Sci. Lett.*, **53**:400–408.

Bukry, D. (1976). Silicoflagellate and coccolith stratigraphy, southeastern Pacific Ocean, Deep Sea Drilling Project Leg 34. **In:** Yeats, R.S., Hart, S.R., et al., *Initial Reports of the Deep Sea Drilling Project*, Vol. 34, U.S. Government Printing Office, Washington, D.C., pp. 715–735.

Bukry, D. (1977). Coccolith and silicoflagellate stratigraphy, central North Atlantic Ocean, Deep Sea Drilling Project Leg 37. **In:** Aumento, F., Melson, W.G., et al., *Initial Reports Deep Sea Drilling Project*, Vol. 37, U.S. Government Printing Office, Washington, D.C., pp. 917–927.

Bukry, D. (1980). Silicoflagellate biostratigraphy and paleoecology in the eastern equatorial Pacific, Deep Sea Drilling Project Leg 54. **In:** Rosendahl, B.R., Hekinian, R., et al., *Initial Reports Deep Sea Drilling Project*, Vol. 54, U.S. Government Printing Office, Washington, D.C., pp. 545–573.

Bukry, D. (1981). Synthesis of silicoflagellate stratigraphy for Maestrichtian to Quaternary marine sediment. *SEPM Spec. Publ. 32*, pp. 433–444.

Bukry, D. and J.H. Foster (1973). Silicoflagellate and diatom stratigraphy, Deep Sea Drilling Project Leg 16. **In:** van Andel, T.H., Heath, G.R., et al., *Initial Reports Deep Sea Drilling Project*, Vol. 16, U.S. Government Printing Office, Washington, D.C., pp. 815–871.

Ciesielski, P.F. (1975). Biostratigraphy and paleoecology of Neogene and Oligocene silicoflagellates from cores recovered during Antarctic Leg 28, Deep Sea Drilling Project. **In:** Hayes, D.E., Frakes, L.A., et al., *Initial Reports Deep Sea Drilling Project*, Vol. 28, U.S. Government Printing Office, Washington, D.C., pp. 625–691.

Dumitrica, P. (1972). Miocene and Quaternary silicoflagellates in sediments from the Mediterranean Sea. **In:** Ryan, W.B.F., Hsu, K.J., et al., *Initial Reports Deep Sea Drilling Project*, Vol. 13, U.S. Government Printing Office, Washington, D.C., pp. 902–933.

Dumitrica, P. (1973a). Paleocene, late Oligocene and post-Oligocene silicoflagellates in southwestern Pacific sediments cored on DSDP Leg 21. **In:** Burns, R.F., Andrews, J.E. et al., *Initial Reports Deep Sea Drilling Project*, Vol. 21, U.S. Government Printing Office, Washington, D.C., pp. 837–883.

Dumitrica, P. (1973b). Cenozoic endoskeletal Dinoflagellates in southwestern Pacific sediments cored during Leg 21 of the DSDP. **In:** Burns, R.F., Andrews, J.E. et al., *Initial Reports Deep Sea Drilling Project*, Vol. 21, U.S. Government Printing Office, Washington, D.C., pp. 819–835.

Dunbar, R.B. and W.H. Berger (1981). Fecal pellet flux to modern bottom sediments of Santa Barbara Basin (California) based on sediment trapping. *Geol. Soc. Amer. Bull., Part I*,**92**:212–218.

Ehrenberg, C.G. (1837). Eine briefliche Nachrict des Hrn. Agassiz in Neuchatel über den ebenfalls aus mikroskopischen Kiesel-Organismen gebildten Polirschiefer von Oran in Afrika. *K. Preuss. Akad. Wiss., Berlin, Verh.*, pp. 59–61.

Ehrenberg, C.G. (1841). Über noch jetzt zahlreich lebende Thierarten der Kreidelbildung und den Organismus der Polythalamien. *K. Akad. Wiss. Berlin, Abh., Jahrg. 1839*, pp. 81–174.

Ehrenberg, C.G. (1854). *Mikrogeologie*, Leopold Voss, Leipzig, pp. 1–xxvii, 1–374.

Ehrenberg, C.G. (1854). *Mikrogeologie, das Erden und Felsen schaffende Wirken des unsichtbar kleinen selbstandigen Lebens auf der Erde.* Leopold Voss, Leipzig, 374 pp.

Haeckel, E. (1861). Uber neue, Iebende Radiolarien des Mittelmeeres. *K. Preuss. Akad. Wiss. Berlin, Monatsber., Jahrg. 1860*, pp. 794.

Haeckel, E. (1862). *Die Radiolarien (Rhizopoda Radiolaris): Eine Monographie*, Georg Reimer, Berlin, xiv + 572 pp.

Haeckel, E. (1887). Reports on the Radiolaria collected by H.M.S. Challenger during the years 1873–1876. *Rept. Voyage Challenger, Zool.*, **18**:1–1803.

Honjo, S. (1978). Sedimentation of materials in the Sargasso Sea at a 5,367 m deep station. *Jour. Mar. Res.*, **36**:469–492.

Honjo, S. (1980). Material fluxes and modes of sedimentation in the mesopelagic and bathypelagic zones. *Jour. Mar. Res.*, **38**:53–97.

Honjo, S., J.F. Connell and P.L. Sachs (1980). Deep ocean sediment trap: design and function of PARFLUX Mark II. *Deep-Sea Res.*, **27**:745–753.

Honjo, S., S.J. Manganini and J.J. Cole (1982). Sedimentation of biogenic matter in the deep ocean. *Deep-Sea Res.*, **29**:609–625.

Hurd, D.C. and S. Birdwhistell (1983). On producing a more general model for biogenic silica dissolution. *Amer. Jour. Science*, **283**:1–28.

Kozlova, O.G. and V.V. Mukhina (1967). Diatoms and silicoflagellates in suspension and floor sediments of the Pacific Ocean. *Internat. Geol. Rev.*, **9**(10):1322–1342.

Lemmermann, E. (1901). Silicoflagellatae. Erhebnisse einer Reise nach dem Pacific. H. Schauinsland 1896/97. *Deutsche Botanische Gesellschaft, Berichte*, **19**:247–271.

Lemmermann, E. (1908). Flagellatae, Chloraphyceae, Coccophaerales und Silicoflagellatae: Klasse Silicoflagellatae. **In:** K. Brandt and C. Apstein (eds.), *Nordisches Plankton, Botanischer Teil*, Vol. 8, pt. 21, pp. 25–32.

Ling, H.Y. (1970). Silicoflagellates from central North Pacific core sediments. *Bull. Amer. Paleontology*, **58**:85–129.

Ling, H.Y. (1973). Silicoflagellates and ebridians from Leg 19. **In:** Creager, J.S., Scholl, D.W., et al., *Initial Reports Deep Sea Drilling Project*, Vol. 19, U.S. Government Printing Office, Washington, D.C., pp. 751–775.

Ling, H.Y. (1975). Silicoflagellates and ebridians from Leg 31. **In:** Karig, D.E., Ingle, J.C., Jr., et al., *Initial Reports Deep Sea Drilling Project*, Vol. 31, U.S. Government Printing Office, Washington, D.C., pp. 763–777.

Ling, H.Y. (1977). Late Cenozoic silicoflagellate and ebridians from the eastern North Pacific region. **In:** *Proceedings of the First International Congress on Pacific Neogene Stratigraphy, Tokyo*, pp. 205–233.

Ling, H.Y. and K. Takahashi (1985). The silicoflagellate genus *Octactis* Schiller, 1925: a synonym of the genus *Distephanus*, *Micropaleontology*, **31**:76–81.

Lipps, J.H. (1970). Ecology and evolution of silicoflagellates. *Proceedings of the North American Paleontology Convention*, pt. G, pp. 965–993.

Lisitzin, A.P. (1971). Distribution of siliceous microfossils in suspension and in bottom sediments. **In:** B.M. Funnell, B.M. and W.R. Riedel (eds.),*Micropaleontology of Oceans*, Cambridge, pp. 173–195.

Locker, S. (1974). Revision der Silicoflagellaten aus der Mikrogeologischen Sammlung von C.G. Ehrenberg. *Ecol. Geol. Helv.*, **67**(3):631–646.

Loeblich, A.R., 3rd, L.A. Loeblich, H. Tappan and Loeblich, A.R., Jr., (1968). Annotated index of fossil and recent silicoflagellates and ebridians with descriptions and illustrations of validly proposed taxa. *Geol. Soc. America Mem. 106*, 319 pp.

Murray, D. and H. Schrader (1983). Distribution of silicoflagellates in plankton and core top samples from the Gulf of California. *Mar. Micropaleontol.*, **7**:517–539.

Nival, P. (1965). Sur le cycle de *Dictyocha fibula* Ehr. dans les eaux de surface de la rade de Villefranche-sur-Mer. *Cah. Biol. Mar.*, **6**:67–82.

O'Kane, J.A., Jr. (1970). *Silicoflagellates of Monterey Bay, California*. M.Sci. Thesis, San Jose State College, 92 pp.

Orr, W.N. and S. Conley (1976). Siliceous dinoflagellates in the northeast Pacific rim. *Micropaleont.*, **22**(1):92–99.

Perch-Nielsen, K. (1978). Eocene to Pliocene archaeomonads, ebridians, and endoskeletal dinoflagellates from the Norwegian Sea, DSDP Leg 38. **In:** Talwani, M., Udintsev, G., et al., *Initial Reports Deep Sea Drilling Project*, Supplement to volumes 38, 39, 40, and 41, U.S. Government Printing Office, Washington, D.C., pp. 147–175.

Poelchau, H.S. (1974). *Holocene silicoflagellates of the North Pacific: their distribution and use for paleotemperature determination*, Ph.D. Thesis, University of California, San Diego, 165 pp.

Poelchau, H.S. (1976). Distribution of Holocene silicoflagellates in North Pacific sediments. *Micropaleont.*, **22**(2):164–193.

Schrader, H.J. and R. Gersonde (1978). Diatoms and silicoflagellates. *Utrecht Micropaleontological Bulletins*, **17**:129–176.

Shitanaka, M. (1983). Silicoflagellate remains in the sediments of Lake Hiruga, Fukui, Japan. *Research Report, Mizunami Fossil Museum*, **10**:171–180 (in Japanese).

Shitanaka, M., F. Ogawa and W. Ichikawa (1970). Silicoflagellate remains in the deep-sea sediments from the Sea of Japan. *Japan Sea*, **4**:1 (in Japanese).

Silver, M.W. and A.L. Alldredge (1981). Bathypelagic marine snow: deep-sea algal and detrital community. *Jour. Mar. Res.*, **39**(3):501–530.

Takahashi, K. (1981). *Vertical flux, ecology and dissolution of Radiolaria in tropical oceans: implications for the silica cycle*, Ph.D. Thesis, Massachusetts Institute of Technology/Woods Hole Oceanographic Institution, 461 pp.

Takahashi, K. (in press). Radiolaria: flux, ecology, and taxonomy in the Pacific and Atlantic. S. Honjo (ed.) *Ocean Biocoenosis Series*.

Takahashi, K. and S. Honjo (1981). Vertical flux of Radiolaria: a taxon-quantitative sediment trap study from the western tropical Atlantic. *Micropaleont.*, **27**(2):140–190.

Takahashi, K. and S. Honjo (1983). Radiolarian skeletons: size, weight, sinking speed and residence time in tropical pelagic oceans. *Deep-Sea Res.*, **30**:543–568.

Thunell, R.C. and S. Honjo (1981). Planktonic foraminifera flux to the deep ocean: sediment trap results from the tropical Atlantic and the central Pacific. *Mar. Geol.*, **40**:237–253.

Thunell, R.C., W.B. Curry and S. Honjo (1983). Seasonal variation in the flux of planktonic foraminifera: time series sediment trap results from the Panama Basin. *Earth Planet. Science Lett.*, **64**:44–55.

Plates

PLATE 1

1, 5, 6 *Dictyocha messanensis messanensis* HAECKEL

1 Station PB_1: 3,791 m, SEM, × 1,100.

5 Station E: 389 m, LM, × 850.

6 Station PB_1: 3,769 m, SEM, × 1,270.

2–4, 15 *Dictyocha messanensis* Haeckel *spinosa* LEMMERMANN

2 Station E: 389 m, LM, × 850.

3 Station PB_1: 2,869 m, LM, × 850.

4 Station PB_1: 3,769 m, SEM,× 940.

15 pentagonal specimen, Station E: 389 m, LM, × 850.

7 *Dictyocha* sp. A
Station P_1: 2,778 m, LM, × 850.

8, 9 *Dictyocha mandrai* LING

8 Station PB_1: 3,769 m, SEM, × 1,100.

9 side view, Station PB_1: 3,769 m, SEM, × 1,160.

10, 11 *Dictyocha* sp. cf. *mandrai* LING
Station E: 389 m, LM, × 850.

12, 13 *Dictyocha calida* POELCHAU

12 Station PB_1: 3,769 m, SEM, × 990.

13 Station PB_1: 2,869 m, LM, × 850.

14 *Dictyocha* sp. B
Station P_1: 2,778 m, LM, × 850.

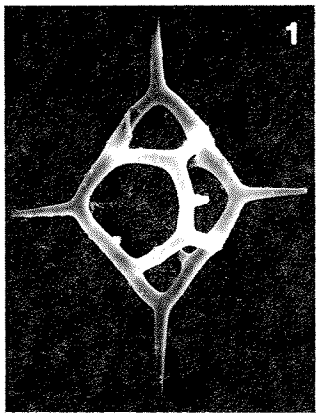
1

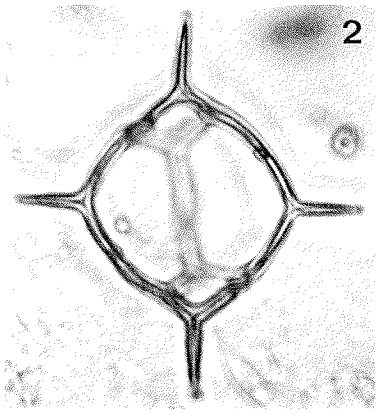
2

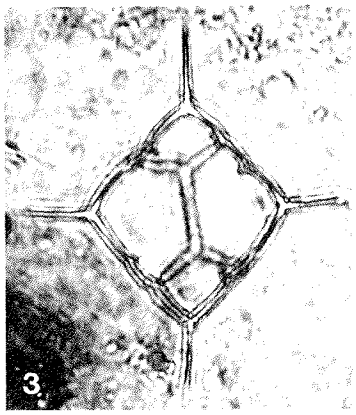
3

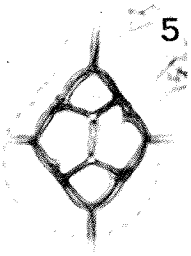
5

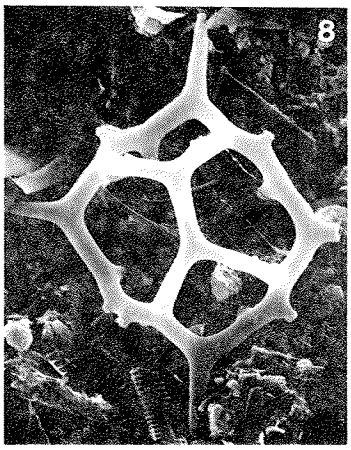
8

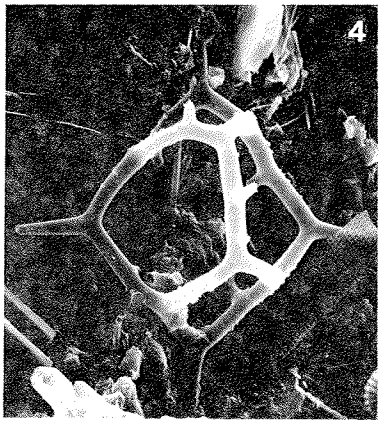
4

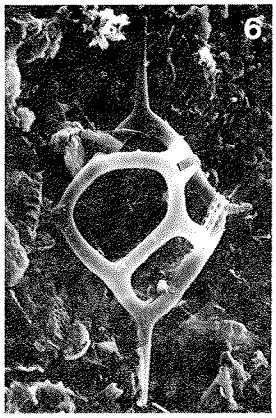
6

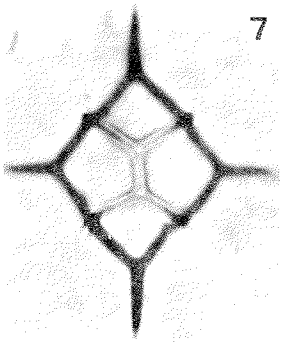
7

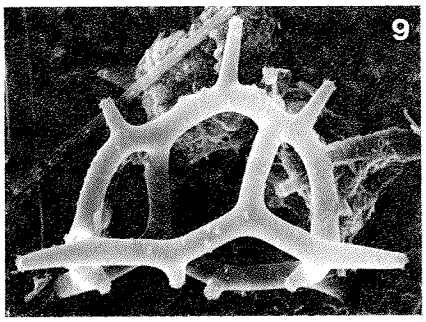
9

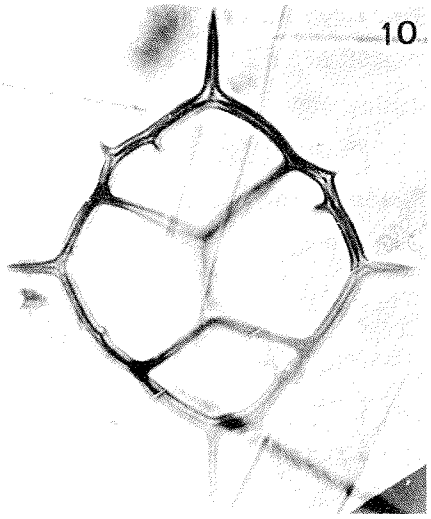
10

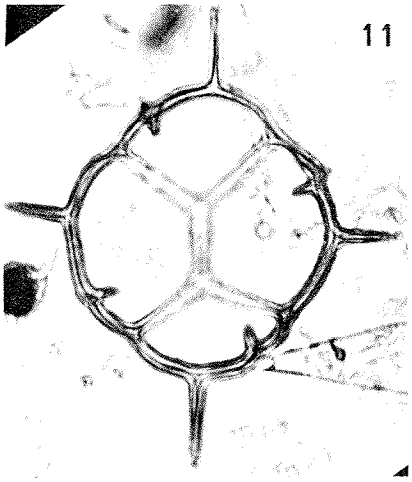
11

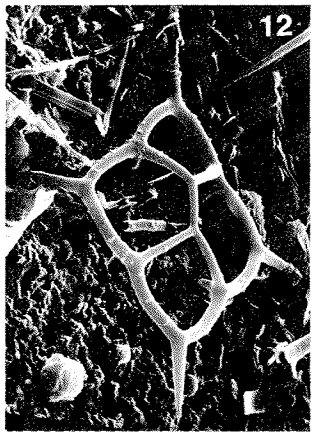
12

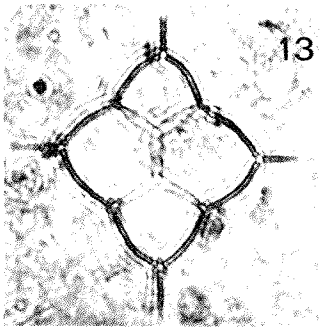
13

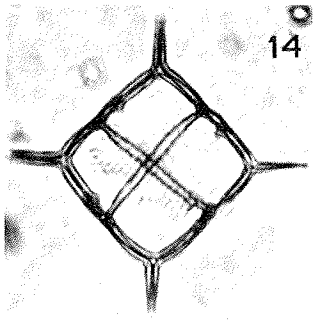
14

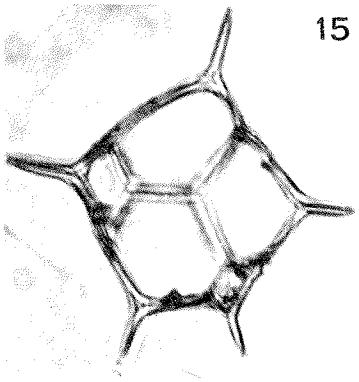
15

PLATE 2

1 *Dictyocha mandrai* LING
pentagonal specimen, Station S_2: 3,394 m, LM, × 850.

2–4 *Dictyocha perlaevis*? FRENGUELLI

2 specimen with an apical window, Station PB_1: 2,869 m, LM, × 850.

3 most common form, Station PB_1: 3,791 m, LM, × 850.

4 elongate form, Station PB_1: 2,869 m, LM,× 850.

5–11 *Distephanus pulchra* (Schiller) LING AND TAKAHASHI

5, 6 Station PB_1: 2,869 m, LM, × 850.

7 Station PB_1: 3,769 m, SEM, × 1,270.

8 large form, Station PB_1: 3,769 m, SEM, × 500.

9 Station PB_1: 3,769 m, SEM, × 990.

10 large and 10-sided form, Station PB_1: 4,280 m, SEM, × 770.

11 Station PB_1: 3,769 m, SEM, × 1,100.

12–15 *Actiniscus pentasterias* (Ehrenberg) EHRENBERG

12 Station PB_1: 3,791 m, SEM, × 1,820.

13 enlarged oblique apical view of specimen shown in figure 12, Station PB_1: 3,791 m, SEM, × 3,700.

14 Station PB_1: 3,769 m, SEM, × 2,370.

15 basal view, Station PB_1: 3,769 m, SEM, × 1,650.

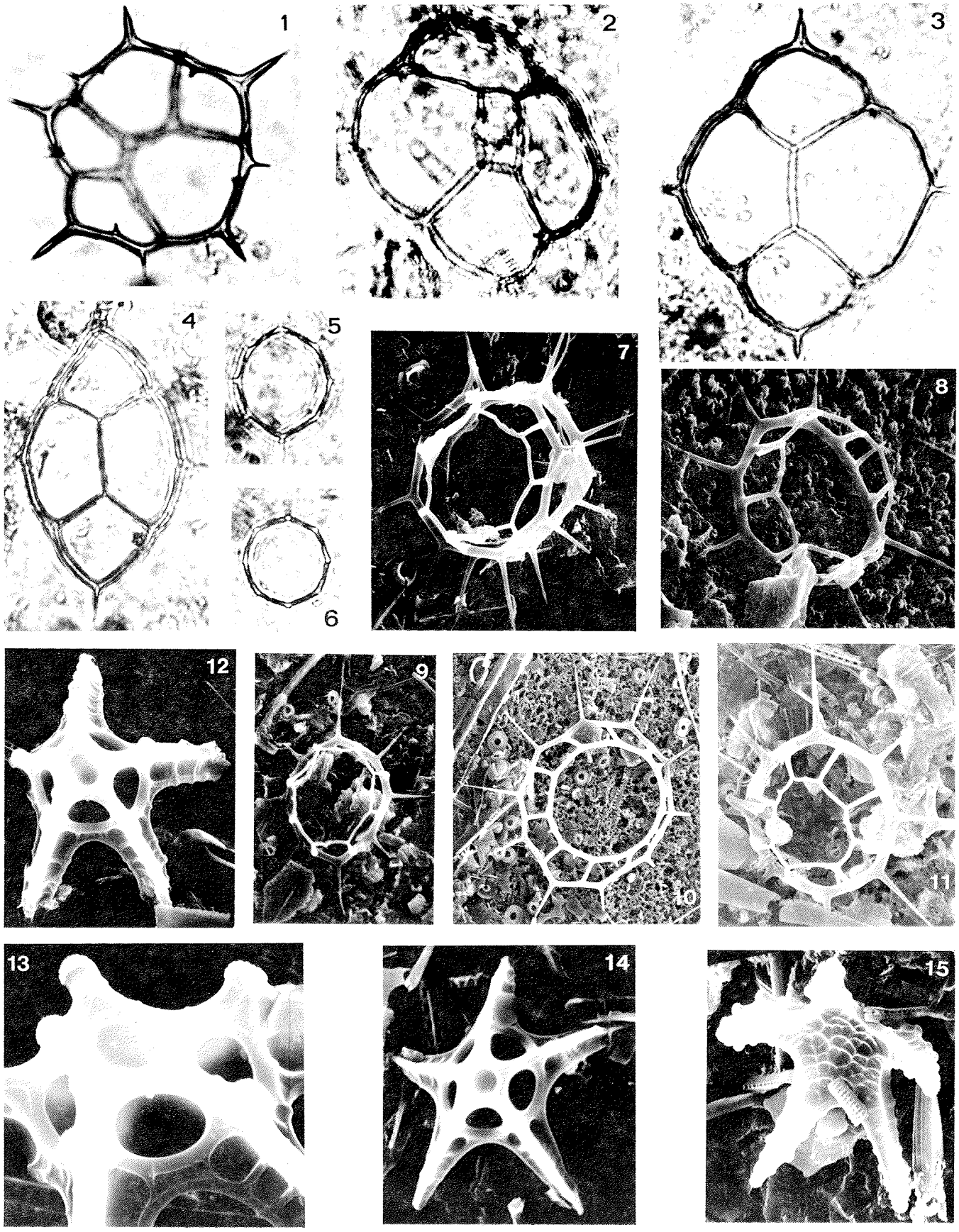
1
2
3
4
5
6
7
8
12
9
10
11
13
14
15